Proceedings of the EuroGNC 2013, 2nd CEAS Specialist Conference
on Guidance, Navigation & Control, Delft University of Technology,
Delft, The Netherlands, April 10-12, 2013

A Low-Cost Integrated System for Indoor and Outdoor Navigation of Miniature UAVs

François-Xavier Marmet, Sylvain Bertrand, Bruno Hérissé and Mathieu Carton

Abstract This paper presents an hardware device and associated algorithms for the navigation of miniature rotorcraft-based Unmanned Aerial Vehicles (UAVs). Unlike many studies that focus on navigation solutions adapted to one single type of mission and environment, the proposed approach aims at simultaneously dealing with indoor and outdoor missions, as well as being robust to sensors' loss and/or faulty measurements. An hardware device with low-cost sensors is presented as well as algorithms that are used to estimate online the vehicle's state composed of its position, attitude and velocities. This estimation architecture, based on complementary and Kalman filters, enables measurement selection and fusion from different sensors, depending on the current environment (indoor or outdoor). Algorithms are described and simulation results are provided to illustrate and compare the performance of the proposed approach.

1 Introduction

Unmanned Aerial Vehicles (UAVs) have been used for the past fifteen years, mainly to the benefit of governmental entities (defence, law enforcement agencies, etc.). While reconnaissance was and still is the prime purpose of UAVs, their outstanding overall capabilities also make them premium candidates for civilian activities such

François-Xavier Marmet
ENAC, 7 avenue Edouard-Belin CS 54005 - 31055 Toulouse Cedex 4, France
e-mail: francois-xavier.marmet@eleve.enac.fr

Sylvain Bertrand and Bruno Hérissé
ONERA, The French Aerospace Lab, F-91761 Palaiseau, France
e-mail: sylvain.bertrand@onera.fr, bruno.herisse@onera.fr

Mathieu Carton
ONERA at the time of the project, The French Aerospace Lab, F-91761, Palaiseau, France
e-mail: mathieu.carton@airbus.com

as, but not limited to, aerial mapping or critical facilities surveillance. Thanks to technological breakthroughs over the past few years, miniaturization and reduction in costs, there has been growing interest in miniature, easy-to-use, cheap, fully autonomous UAVs, able to operate indoors as well as outdoors. Rotorcraft-based vehicles are especially widely used thanks to their vertical take-off and landing (VTOL) and stationary flight capabilities.

To control these vehicles and make them autonomous, information such as attitude angles, velocities (linear and angular), position, localization wrt environment, etc., are required during the flight. Such information can be computed by navigation algorithms from measurements provided by on board sensors. Measurements provided by IMU sensors are widely used to estimate attitude angles [11, 13]. These can be combined with GPS data in outdoor environments to recover for position and velocities [8, 17, 18]. Artificial beacons such as external cameras have also been used [14]. For indoor environments, information provided by exteroceptive sensors can be used to localize the vehicle. Visual methods such as visual SLAM have been experimented successfully [2]. SLAM techniques have also been implemented using a laser range finder sensor [1, 7]. External positioning systems based on ultrasonic sensors have also been developed for indoor localisation [4].

Most of these work focus on navigation problems for UAVs, regarding to a given application, or to a given type of mission in a given environment. However, miniature UAVs can be used in very different and/or changing environments during a given mission. Depending on these conditions of use, measurements provided by on board sensors can be available or not during the flight for navigation. For example, the beginning of the mission can take place in an outdoor environment, where GPS signal is available. During the mission, the vehicle can enter a building, where the same signal would not be available any more, but where distance measurements to indoor walls could be provided by on board telemeters. It is therefore of interest to develop a navigation solution that can handle different situations without compromising the mission. Some recent work address this issue by proposing vision-based solutions [5, 15].

In this paper, the development of an hardware device based on low-cost sensors and associated algorithms is presented for indoor and outdoor navigation of miniature rotorcraft UAVs without using vision-based solutions. The proposed approach aims at enabling measurement selection and fusion from the different on-board sensors, depending on the current environment (indoor or outdoor), and being robust to sensors' loss and/or faulty measurements. Test and simulation results are provided to illustrate the performance of the proposed approach in operational situations.

The paper is organized as follows: Section 2 presents the hardware device and gives a high-level description of the state estimation architecture. Section 3 focuses on the attitude estimation algorithm, based on a complementary filter. Section 4 deals with position and velocity estimation using Kalman filtering and selection of measurements provided by the sensors. Simulation results are provided in Section 5 and concluding remarks as well as directions for future work are provided in the last section of the paper.

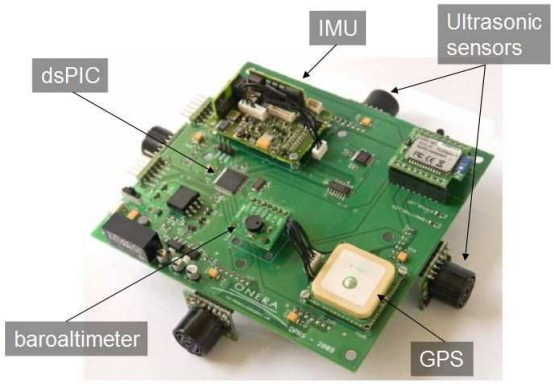

Fig. 1 Hardware device. The overall cost of the device is about 2.5k Euros. Total mass is 110g, dimensions are 11.5cm by 12.5 cm and current consumption is 180mA.

2 Hardware and Estimation Architecture

2.1 Hardware Architecture

2.1.1 Hardware device

The hardware device developed in this study was designed under the following guidelines: use of low-cost, commercial off-the-shelf components; overall mass and volume must be kept low, to allow integration to UAVs whose size and mass are respectively a few tens of centimetres and a kilogram or less; power consumption must be kept low, otherwise jeopardizing endurance of the vehicle. Selected sensors, fitted on the ad hoc PCB, are depicted in Figure 1. A dsPIC has been chosen, and a wireless connexion can be used to allow data downlink to a ground station, if required.

2.1.2 Description of sensors

The following sensors have been integrated on the developed hardware device:

Inertial Measurement Unit (IMU): Xsens MTi strapdown IMU with nine MEMS sensors (three accelerometers, three rate gyros and three magnetometers) and 100Hz measurement frequency. Measurements are mainly impaired by random, time-dependent biases and noise.

GPS receiver: a LocoSys LS20031 GPS receiver has been chosen. 3D position, DOP indicators, ground speed and heading relative to true North are delivered at 5Hz. No raw data are available. Measurements are mainly impaired by noise and a bias.

Ultrasonic sensors: Maxbotix ultrasonic sensors provide relative distance measurements at 20Hz. Their range is limited (from 15cm to 6.5m). Up to six sensors can be simultaneously used (eg. four sensors pointing to front-back-left-right directions of the vehicle and two sensors pointing to top-down directions).

Baroaltimeter: a VTI SCP1000-D01 baroaltimeter provides pressure measurements at 1.8Hz which are converted into altitude.

2.2 Estimation architecture

2.2.1 Estimation problem, notations and assumptions

The estimation problem consists in computing, from available sensor measurements, the state of the vehicle composed of its position coordinates, orientation angles, and velocities components (linear and angular). This set of data can be used for navigation (localisation and mission planning) as well as for guidance and control of the vehicle. Therefore, it must be accurate and computed at a period smaller than the time constant of the vehicle dynamics.
To introduce the architecture and algorithms used for solving this estimation problem, some notations are introduced.

Reference frames: The following reference frames are considered:

- $\mathscr{R}_i$: Earth centred inertial frame,
- $\mathscr{R}_e$: Earth centred Earth fixed frame (ECEF),
- $\mathscr{R}_n$: local navigation frame, of reference O, associated with the vector basis (e_N, e_E, e_D) pointing to North, East and Downwards directions,
- $\mathscr{R}_b$: body frame attached to the vehicle, of reference G (centre of mass of the vehicle), associated with the vector basis (e_1^b, e_2^b, e_3^b) where e_1^b is directed along the longitudinal axis of the vehicle and pointing to its front, e_2^b is directed along the lateral axis and pointing to its right, and e_3^b is directed along the vertical axis of the vehicle and pointing to its bottom.

Kinematics: The position and the linear velocity of the vehicle in $\mathscr{R}_n$ will be respectively denoted by $r = [r_N \;\; r_E \;\; r_D]^T$ and $v = [v_N \;\; v_E \;\; v_D]^T$. The rotation matrix from $\mathscr{R}_b$ to $\mathscr{R}_n$ will be denoted by $R \in SO(3)$. It defines the orientation of the vehicle which can also be parametrized by Euler's angles ψ (yaw), θ (pitch) and ϕ (roll). The notation $\omega_{jk} \in \mathbb{R}^3$ (with $k, j \in \{i, e, n, b\}$) will be used to denote the angular velocity of $\mathscr{R}_j$ wrt $\mathscr{R}_k$. For simplicity the notation $\omega = \omega_{nb}$ will be used.

Measurements: The subscript $\cdot_{meas}$ will be used to denote measured quantities. The following models have been chosen to model measurements provided by the IMU sensors. It has been assumed that errors due to scale factors and misalignments can be neglected, provided a precise positioning and calibration of the IMU and com-

pensation of known manufacturing errors.

Accelerometers:

$$f_{meas} = f + b_f + n_f \tag{1}$$

where $f \in \mathbb{R}^3$ is the specific force, $b_f \in \mathbb{R}^3$ the accelerometer constant bias and $n_f \in \mathbb{R}^3$ a zero mean Gaussian white noise of covariance matrix $Q_f = \text{diag}(\sigma_{fx}^2, \sigma_{fy}^2, \sigma_{fz}^2)$.

Rate gyros:

$$\omega_{meas} = \omega + b_\omega + n_\omega \tag{2}$$

with $b_\omega \in \mathbb{R}^3$ rate gyro the constant bias and $n_\omega \in \mathbb{R}^3$ a zero mean Gaussian white noise of covariance matrix $Q_\omega = \text{diag}(\sigma_{\omega x}^2, \sigma_{\omega y}^2, \sigma_{\omega z}^2)$.

Assumptions: The two following assumptions are considered for the estimation problem and the design of the associated algorithms.

Assumption 1 *The UAV is supposed to be used for missions within a kilometer range.*

As a consequence, the Earth is considered to be flat and its rotation is neglected. Therefore it can be assumed that $\omega_{ie} = 0$ and $\omega_{en} = 0$. In addition, the gravity is assumed to be constant and is expressed by $g = [0, 0, -g_0]^T$ in $\mathscr{R}_n$, with $g_0 = 9.81$ m.s^{-2}.

Assumption 2 *The UAV is supposed to be used in quasi-stationary flight conditions.*

This assumption is verified for rotorcraft-based miniature UAVs flying at low speed and not performing acrobatic manoeuvres.

2.2.2 Estimation architecture description

For miniature UAVs a strapdown IMU is typically used to provide measurements at a high frequency that will be processed to estimate attitude, position and velocities of the vehicle. Based on inertial navigation equations, an Inertial Navigation System (INS) can hence be developed to compute these estimates [6, 16]. Nevertheless, components of low-cost IMUs suffer from important bias which, once integrated by the INS, lead to significant drifts and even divergence in the computed estimates. It is therefore necessary to correct the estimates by using additional sensors providing "external" measurements. Such sensors are typically GPS and baro-altimeter [9]. External information can hence be added in the estimation process to correct position and velocity components predicted by the INS.
Note that the estimation architecture of [9] has been used as starting point for developments proposed in this paper and will be used as reference for performance comparison. This estimation architecture is based on an INS along with a Kalman

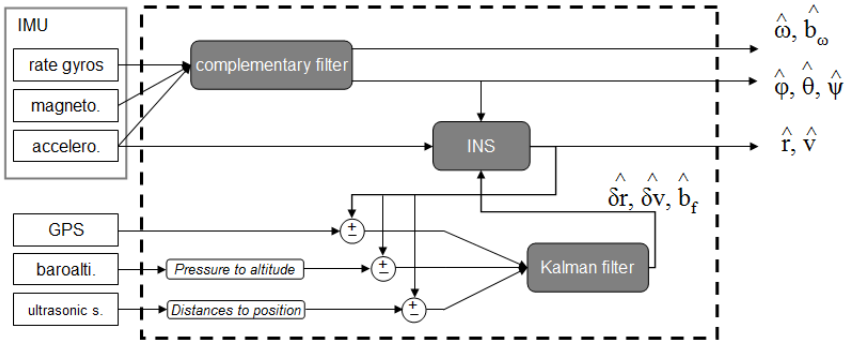

Fig. 2 Estimation architecture

filter used in indirect integration form and direct feedback.
In this paper, measurements provided by ultrasonic sensors are also considered. In outdoor environments, ultrasonic sensors directed along the "vertical" axis of the vehicle frame are used to provide altitude measurements, when flying at low altitude. In indoor environments, where use of GPS can prove to be difficult, ultra sonic sensors along the "longitudinal" and "lateral" axes of the vehicle frame also provide information on other components of the vehicle's position in an environment which geometry is known. In this latter case, it is assumed that the geometry of the environment is well known.
The estimation architecture proposed in this paper is presented in Figure 2. It is composed of three main stages:

- a complementary filter estimates the attitude and angular velocity components of the vehicle and rate gyros' biases, based on measurements provided by IMU's sensors,
- an INS computes estimates of the position and linear velocity components, based on attitude information provided by the complementary filter, and position and velocity corrections provided by a Kalman filter,
- a Kalman filter computes corrections in position and linear velocity components and estimation of accelerometers' biases, based on estimates provided by the INS and measurements from GPS, baroaltimeter and ultrasonic sensors.

The INS and Kalman filter part of the estimation architecture is designed as a multi-rate, multi-sensor structure with an indirect integration form and direct feedback. This implies that the propagated states in the Kalman filter are position and linear velocity errors, i.e. differences between values estimated by the INS and measurements provided by "external" sensors. The state transition model is therefore the model of inertial navigation equations' errors, which can be assumed to remain linear as long as the errors are small enough (which justifies the choice of direct feedback, guaranteeing that the INS errors remain small and bounded). Since the Kalman filter is used to compute corrections, it can operate at a much slower rate than the IMU's one, making it computationally reasonable.

To add robustness with respect to erroneous and/or perturbed measurements, a fuzzy logic approach has been adopted in both the complementary and Kalman filter stages to select measurements to be considered from all the ones given as input. Sensors used to provide the measurements given as inputs to the Kalman filter are chosen previously depending on the environment.

The next sections of this paper are devoted to a more precise description of the algorithms used in the estimation architecture.

3 Attitude estimation

The problem is to estimate the orientation matrix R of the vehicle from measurements delivered by the IMU's sensors: 3 axes rate gyros, 3 axes accelerometers and 3 axes magnetometers. Under Assumption 2, accelerometers can be used as inclinometers since the gravity component dominates the total acceleration vector. Therefore, it can be assumed that accelerometers provide a measurement $\eta_a \in \mathbb{R}^3$ of the local vertical. The magnetometers provide a second reference vector $\eta_m \in \mathbb{R}^3$ corresponding to Earth magnetic field. Since only the direction of these vectors is used, η_a and η_m are defined as unit vectors. These vectors can be written as follows:

$$\eta_a = R^\top \eta_{a0} + n_a \tag{3}$$

$$\eta_m = R^\top \eta_{m0} + n_m \tag{4}$$

where $\eta_{a0} \in \mathbb{R}^3$ and $\eta_{m0} \in \mathbb{R}^3$ are the reference vectors expressed in $\mathscr{R}_n$ and $n_a \in \mathbb{R}^3$ and $n_m \in \mathbb{R}^3$ are noises. Rate gyros provide a measure ω_{meas} of the angular velocity ω expressed in $\mathscr{R}_b$ by (2). Based on this model, the complementary filter presented in [10] has been used:

$$\dot{\hat{R}} = \hat{R}\,\mathrm{sk}\big(\big(\omega_{\text{meas}} - \hat{b}_\omega\big) + k_x\tilde{x}\big) \tag{5}$$

$$\dot{\hat{b}}_\omega = -k_b\tilde{x} \tag{6}$$

$$\tilde{x} = k_a\,(\eta_a \times \hat{\eta}_a) + k_m\,(\eta_m \times \hat{\eta}_m) \tag{7}$$

where $\mathrm{sk}(u)$ denotes the skew-symmetric matrix associated to the vector cross product $\mathrm{sk}(u)x = u \times x$ for a given $u \in \mathbb{R}^3$ and for any $x \in \mathbb{R}^3$. $\hat{R}$ and $\hat{b}_\omega$ denote the estimates of R and b_ω respectively, $\hat{\eta}_a = \hat{R}^\top \eta_{a0}$ and $\hat{\eta}_m = \hat{R}^\top \eta_{m0}$.

According to the confidence in measures η_a and η_m, the weights k_a and k_m can be tuned online. For instance, in the case of electromagnetic perturbations, k_m should be chosen such that $k_m \ll k_a$. To deal with this problem, a method using fuzzy logic is proposed in the next subsection.

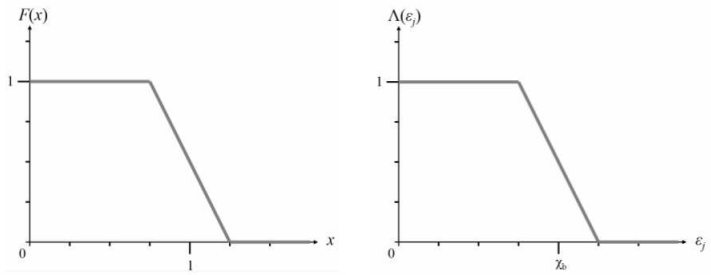

Fig. 3 Function F used for the tuning of gains k_a and k_m, and evolution of weighting factor Λ wrt ε_j (see Section 4.3)

3.1 Robustness to perturbations

In this section, a fuzzy logic approach is used to modulate the weights k_a and k_m according to the degree of confidence in measurements. It consists in using a function F which the value tends to 1 if measurements can be considered valid, and tends to 0 if they cannot. For example, the function can be defined as in Figure 3.

To determine whether a measure is valid or not, a quantitative criterion must be defined:

- The accelerometers can be used as inclinometers if $\|f_{\text{meas}}\| \approx \|g\|$.Therefore, one possible criterion is $\delta_a = |\|f_{\text{meas}}\| - \|g\||$, and the weight k_a can be defined by $k_a = k_{a0}\,\mathrm{F}\left(\frac{\delta_a}{\delta_{a0}}\right)$ where δ_{a0} is a threshold and k_{a0} the maximum value of k_a.
- Analogously to the accelerometers, the criterion for the magnetometers can be chosen as $\delta_m = |\|H_{\text{meas}}\| - \|H_e\||$ where H_{meas} is the measured magnetic field and H_e is the Earth's magnetic field. The weight k_m can be defined by $k_m = k_{m0}\,\mathrm{F}\left(\frac{\delta_m}{\delta_{m0}}\right)$ where δ_{m0} is a threshold and k_{m0} the maximum value of k_m.

This approach was implemented and tested with the XSens IMU. In the experiment depicted in Figure 4, the IMU sits motionless, θ and ϕ are null, and ψ is equal to 48deg. Five seconds after the initial time, strong electromagnetic (E. M.) perturbations are applied to the XSens IMU (magnetometers at saturation level). Note that the yaw estimation relies solely on magnetometers data, contrary to roll and pitch estimations. The yaw value provided by the complementary filter is compared to the one provided by XSens embedded attitude estimator.

XSens solution errors reach up to 25deg, and takes some time to recover from E.M. perturbations. On the contrary, the complementary filter solution is affected only at the onset of E.M. perturbations, while estimation error never exceeds 2.5 deg (standard deviation of about 1deg).

Robustness to strong accelerations (e.g. caused by wind gust) was also asserted

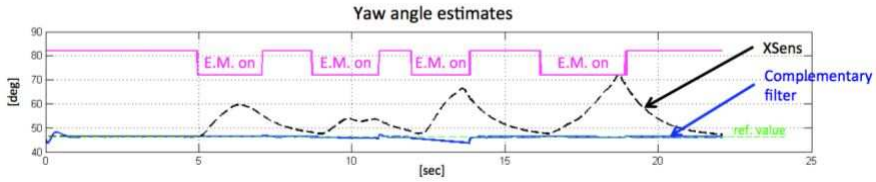

Fig. 4 Yaw estimation in presence of strong electromagnetic (E.M.) perturbations

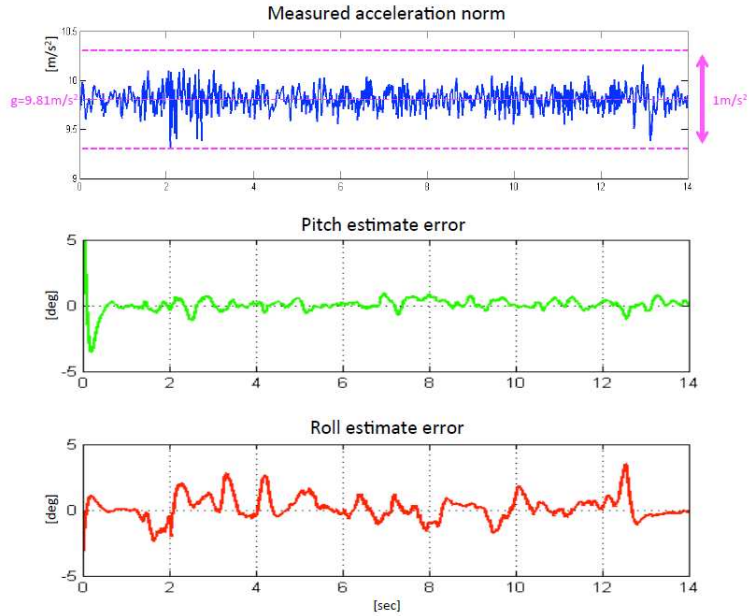

Fig. 5 Pitch and roll estimation in presence of strong accelerations

in regard of validity of Assumption 2. The IMU was moved quite vigorously on a horizontal plane, along its *y* axis. Accelerations in this direction are expected to cause the apparent vertical seen by accelerometers to rotate along the *x* axis in the (*y*,*z*) plane, thus inducing a "false roll". Figure 5 depicts the roll and pitch angles' estimates, along with the norm of the total acceleration seen by accelerometers. The norm has a 1m/s^2 p.t.p. variation, expressing an approximate 3m/s^2 p.t.p. variation along the *y* axis. Pitch and roll errors never exceed 3.0deg (with standard deviation $\leq$1deg), thus proving good robustness to brutal accelerations.

4 Position and velocity estimation

Position and linear velocity are first estimated by the INS using classical strapdown equations for inertial navigation. As previously stated, these estimates are then corrected by using information provided by external sensors.

4.1 Inertial Navigation System

Classical inertial navigation equations can be found in [16] for strapdown IMUs. Simplified equations will be used in this paper based on Assumption 1. The translational dynamics in $\mathscr{R}_n$ are described by

$$\dot{r} = v \tag{8}$$

$$\dot{v} = Rf + g \tag{9}$$

and orientation dynamics in $\mathscr{R}_b$ by

$$\dot{R} = R\,\mathrm{sk}(\omega_{nb}) \tag{10}$$

Using angular velocity composition $\omega_{nb} = \omega_{ne} + \omega_{ei} + \omega_{ib}$ along with Assumption 1, it can be deduced that $\omega_{nb} = \omega_{ib} = \omega$ and equation (10) becomes:

$$\dot{R} = R\,\mathrm{sk}(\omega) \tag{11}$$

A classical INS would implement these equations to compute estimated values of the position, attitude and velocity of the vehicle. In this paper, attitude determination is achieved separately by the complementary filter as described in Section 3. The implemented INS structure is therefore based on equations (8) and (9) where the orientation matrix R is directly computed from the attitude estimated by the complementary filter.
As previously stated, these estimates require corrections. Corrections on position and on linear velocity are directly achieved in the INS, in a direct feedback approach as explained in Section 2.2.2. These corrections are estimated by a Kalman filter, based on measurements provided by external sensors. The direct feedback approach enables to ensure that the estimation of inertial errors remain small and bounded, hence making possible the use of a linear filter as described in the next section.

4.2 Correction with Kalman Filtering and External Sensors

A filter is used to compute estimation errors due to the INS based on measurements of external sensors. As previously stated, it can be assumed that these errors remain small enough to use a linear filter. Therefore, a Kalman filter has been typically chosen in this paper. Prediction state model represents the error dynamics of the INS estimates. Assuming that the complementary filter delivers precise enough attitude estimates, errors on the orientation are not taken into account in the filter design. However, estimation of the accelerometers' biases is considered.

4.2.1 Prediction model

Let us denote by $\delta r = \hat{r} - r$ the position error and by $\delta v = \hat{v} - v$ the error on the linear velocity. Assuming that estimation of the orientation matrix R and of the gravity g are not affected by errors, the error dynamics is given by:

$$\delta \dot{r} = \delta v \tag{12}$$

$$\delta \dot{v} = R\,(f_{meas} - f) \tag{13}$$

Using (1) equation (13) becomes:

$$\delta \dot{v} = R\,b_f + R\,n_f \tag{14}$$

Let us assume that the accelerometer bias can be described by a first order model [16]:

$$\dot{b}_f = -T_f^{-1} b_f + n_{b_f} \tag{15}$$

with $T_f \in \mathbb{R}^{3\times 3}$ a diagonal matrix of time constants.

Denoting by t_e the sampling period, let us define at time $t_k = k t_e$ the state vector $X(k) = \left[\delta r(k)^T \;\; \delta v(k)^T \;\; b_f(k)^T\right]^T$ and the noise vector $N(k) = \left[n_p(k)^T \;\; n_f(k)^T \;\; n_{b_f}(k)^T\right]^T$. A discrete-time model of the form $X(k+1) = A(k)X(k) + B(k)N(k)$ equivalent to (12)-(14)-(15) can be derived, where $A(k)$ and $B(k)$ are computed using [12]. The covariance matrix of $N(k)$ is given by $Q = \mathrm{diag}(\sigma_{p_x}^2, \sigma_{p_y}^2, \sigma_{p_z}^2, \sigma_{f_x}^2, \sigma_{f_y}^2, \sigma_{f_z}^2, \sigma_{b_{fx}}^2, \sigma_{b_{fy}}^2, \sigma_{b_{fz}}^2)$ and is considered to be time-invariant.

4.2.2 Measurement model

Let $m(k)$ be the number of measurements available at time k. Define by $Y(k) = \left[Y_1(k)...Y_{m(k)}(k)\right]^T \in \mathbb{R}^{m(k)}$ the vector composed of all available measurements $Y_i(k) \in \mathbb{R}$ $(i = 1,..,m(k))$. The measurement equation is defined as $Y(k) = C(k)X(k) + W(k)$ with

$$C(k) = \begin{bmatrix} C_1(k) \\ ... \\ C_{m(k)}(k) \end{bmatrix} \text{ with } C_i(k) \in \mathbb{R}^{1\times 9} \quad (i = 1,..,m(k)) \tag{16}$$

and where $W(k) \in \mathbb{R}^{m(k)}$ is a noise vector of covariance matrix $\Re(k) = \text{diag}(R_1(k),\ldots,R_{m(k)}(k))$ where $R_i(k)$ $(i = 1,..,m(k))$ is the covariance matrix corresponding to measurement $Y_i(k)$.
Up to ten measurements can be available at a given iteration: position measurement provided by GPS, altitude measurement from baro-altimeter and "pseudo-measurements" in position from ultrasonic sensors.

4.3 Selection of measurements

If an erroneous measurement is provided by one sensor, the estimation accuracy can be strongly affected. One simple way to prevent the use of erroneous observations is to take advantage of the statistical properties of the Kalman filter's innovation.
Let us denote by $\iota_i(k)$ the innovation associated to a subset j of measurements at iteration k, and by $\varepsilon_j(k) = \iota_j(k)^T S_j^{-1}(k)\iota_j(k)$ the corresponding normalized innovation squared, where $S_j(k) = C_j(k)P_{k|k-1}C_j(k)^T + R_j(k)$ is the innovation covariance matrix and $P_{k|k-1}$ the covariance matrix of the predicted state at time k provided by the Kalman filter. The quantity $\varepsilon_j(k)$ follows a χ^2 distribution whose number of degrees of freedom is the dimension of $\iota_j(k)$ [3]. A χ^2 table can hence be used to determine a validity domain for this subset of measurements, for a given confidence level (a value of 95% has been considered). If $\varepsilon_j(k)$ is beyond the boundary χ_b of this domain, the subset of measurement should hence be rejected and not taken into account in the Kalman filter. Note that this approach assumes a good validity of the prediction model.
This method is particularly useful in the case of GPS multipath or mask effects for which measurements should not be taken into account.

Rejecting the subset j of measurements can be achieved by setting their associated covariances to infinity. Instead of using a binary logic approach consisting in completely rejecting the considered subset of measurements, a fuzzy logic approach has been chosen. Covariances of the subset j of measurements are therefore divided by a weighting factor Λ^2 which value is defined according to Figure 3.

4.4 Position Pseudo-Measurements with Ultrasonic Sensors

Distance measurements are given by ultrasonic sensors and thus require processing to compute "pseudo measurements" in position components to be provided to the Kalman filter.

Using Assumption 2, one can consider that attitude angle will be small enough to make the two "vertical" ultrasonic sensors pointing to the ground and to the ceiling for indoor use, and the four "horizontal" ultrasonic sensors pointing to walls for indoor use. Therefore altitude determination is separated from computation of the position's horizontal components.

4.4.1 Geometrical description

Les us denote by C_i the ultrasonic sensor i. The subscript i is used to refer to sensors respectively pointing to the front ($i = f$), to the back ($i = b$), to the left ($i = l$), to the right ($i = r$), "upwards" ($i = u$) and "downwards" ($i = d$) of the vehicle. The position of each sensor c_i in $\mathscr{R}_b$ will be denoted by $r_{C_i} \in \mathbb{R}^3$. It is assumed to be perfectly known, as well as the unit vector $n_{C_i} \in \mathbb{R}^3$ defining the measurement direction of the sensor in $\mathscr{R}_b$. The distance measurement provided by a sensor C_i will be denoted by d_i^{meas}.

4.4.2 Altitude

From distance measurement d_d^{meas} of sensor C_d pointing "downwards", the altitude r_D of the vehicle can be computed by:

$$r_D = -d_d^{meas} \left[n_{C_d}\right]_{\mathscr{R}_n} \cdot e_D - \left[r_{C_d}\right]_{\mathscr{R}_n} \cdot e_D - h \tag{17}$$

where h is equal to the altitude of the local ground with respect to $\mathscr{R}_n$ (altitude of the room in the case of indoor flight, zero in the case of outdoor flight), assumed to be known.

For indoor use, assume that the UAV flies in a room which ceiling is at an height H above the ground. In that case, the altitude r_D can also be computed from distance measurement d_u^{meas} of the sensor pointing "upwards":

$$r_D = -d_u^{meas} \left[n_{C_u}\right]_{\mathscr{R}_n} \cdot e_D - \left[r_{C_u}\right]_{\mathscr{R}_n} \cdot e_D - h - H \tag{18}$$

Note that in (17) and (18) coordinates of n_{C_d}, n_{C_u}, r_{C_d} and r_{C_u} in $\mathscr{R}_n$ (denoted by $[.]_{\mathscr{R}_n}$) are computed using attitude angles provided by the complementary filter.

If measurements d_d^{meas} and d_u^{meas} are both available, coherence of the two values computed from (17) and (18) is verified, and an average altitude value is provided to the Kalman filter.

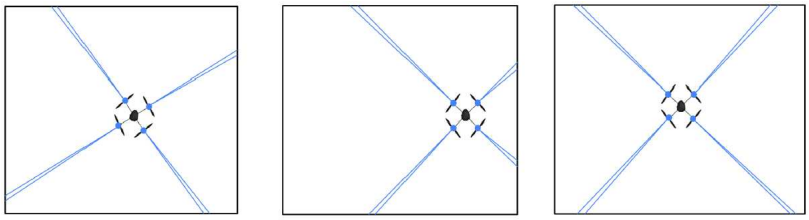

Fig. 6 Three types of configurations of ultrasonic sensors wrt walls (quadrotor vehicle example)

4.4.3 Horizontal components of position

For indoor flights, "horizontal" ultrasonic sensors can be used to compute the r_N and r_E components of the position, assuming the vehicle is in a room which dimensions are known. Depending on the position and orientation of the vehicle in the room, twenty four measurement configurations could be listed, divided into three types as presented on Figure 6. Assuming that the orientation of the vehicle with respect to the room is known, this list of twenty four possible configurations is reduced to seven. Note that for configurations of type 3, a singularity arises and only one of the two horizontal components of the position can be computed.

The following approach has been developed to compute the horizontal components of position from these seven possible configurations:

- *Step 1:* For each configuration where measurement of each sensor i corresponds to a different wall j of the room:
  - The horizontal components r_N and r_E of the position are computed by solving a set of equations of the form (19) using a least square approach, assuming r_D is known.
$$(r + [r_{C_i}]_{\mathscr{R}_n}) \cdot n_{w_j} = k_{w_j} - d_i^{meas} [n_{C_i}]_{\mathscr{R}_n} \cdot n_{w_j} \tag{19}$$
    where n_{w_j} is the normal unit vector of wall j expressed in $\mathscr{R}_n$ and where k_{w_j} defines the plane equation representing wall j in $\mathscr{R}_n$ coordinates by $[\xi]_{\mathscr{R}_n} \cdot n_{w_j} = k_{w_j}$ for any $\xi \in \mathbb{R}^3$.
  - Consistency of each solution is then verified by checking the validity of "measurements" computed from the position components of the solution wrt the true measurements.
  - Consistent solutions are kept.
- *Step 2:* For each configuration where measurements of two sensors i correspond to a same wall j of the room:
  - The horizontal component r_N (respectively r_E) is computed as an average value of the solutions of two equations similar to Step 1, assuming r_E (respectively r_N) and r_D are known.

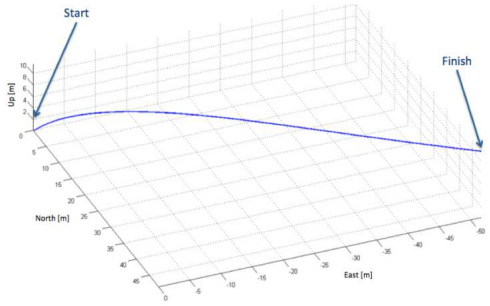

Fig. 7 Simulated trajectory of a quadrotor vehicle (position coordinates in $\mathscr{R}_n$)

– Consistency of the solution is checked as in Step 1.
– Consistent solutions are kept.

Due to sensor low precision and measurement errors, several configurations can provide consistent solutions. In that case, the two configurations that produce the closest solutions are considered. If they prove to be consistent with the position of the UAV computed at the previous time step, an average position is computed and is provided to the Kalman filter.

5 Numerical results

Simulation results for a quadrotor vehicle are presented to illustrate the performance of the proposed approach. These results have been obtained using a simulation tool developed for this study and based on a precise emulation of the quadrotor UAV dynamics (electro-mechanical and aerodynamic models), the environment (geographical position, local magnetic deviation, buildings) and the on-board sensors (accurate models with identification of the parameters based on experiments performed on the sensors of Section 2.1.2).

5.1 Flight setup

Figure 7 presents the simulated flight trajectory. Simulation begins at take-off (reference position of coordinates $[0\ 0\ 0]^T$), and lasts 20 sec. Take-off is set at the center of a location surrounded by walls (no ceiling). These walls form a square (each side having a length of 100m) and are 15m high. Ultrasonic sensors can therefore get out of or in range (max. range is 6.5m), while GPS signals are assumed to be always available (but possibly from a reduced set of visible satellites). The only magnetic perturbations considered come from the running UAV engines.
Estimation results are provided at 100Hz.

5.2 Estimation results

Simulation results are provided for the proposed estimation architecture and are compared to three other architectures. The following notations will be used to refer to these estimation architectures:

- "*INS*": classical INS system using only inertial measurements,
- "*INS+KAL*": estimation architecture of [9] based on INS and Kalman filtering using GPS and baroaltimeter measurements,
- "*UP.INS+KAL*": upgraded version of the estimation architecture of [9] taking into account measurements of ultrasonic sensors,
- "*PEA*": proposed estimation architecture as described in Sections 2.2.2, 3 and 4.

For each estimation architecture, the following quantities are presented: position estimation error, linear velocity estimation error, attitude estimation errors, accelerometers biases estimates (*PEA* only) and rate gyro biases estimates (*PEA* only).

5.2.1 Position, linear velocity and attitude

Position estimation errors are presented in Figure 8. The *INS* solution is mostly nonsensical, due to the quick and strong divergence of integrated measurements from such low-cost inertial components. The same remark applies for both velocity and attitude estimations.
The *UP.INS+KAL* solution shows marginal improvements compared to the original architecture *INS+KAL*. The main benefit of ultrasonic sensors integration is to avoid divergent behaviors, like the one starting at 14 sec for East component of the position estimation error. The *PEA* solution is clearly the best, with a maximum position error of $\pm$3m on any axis. This is mainly explained by the way measurements are used in the estimation process, but also by the very good attitude estimation (see Figure 10). The attitude estimation indeed directly impacts the way IMU's acceleration values are projected along $\mathscr{R}_n$ axes.

Comments about velocity estimation errors presented in Figure 9 are quite similar to the ones regarding estimation of position. The linear velocity estimation error provided by the *PEA* solution never exceeds $\pm$0.5m/s (i.e. 5% of maximum velocity in this simulation).

Attitude estimation results of Figure 10 call for some interesting conclusions. The *INS+KAL* and *UP.INS+KAL* solutions perform even worse than the *INS* solution. This stems from the facts that in these two solutions the Kalman filter tries to estimate attitude corrections (see [9] for more details) without being helped by any direct attitude measurement.
On the contrary, *PEA* attitude is determined by the complementary filter with bias estimation, showing excellent results. Estimation errors on attitude angles never exceed $\pm$0.5deg.

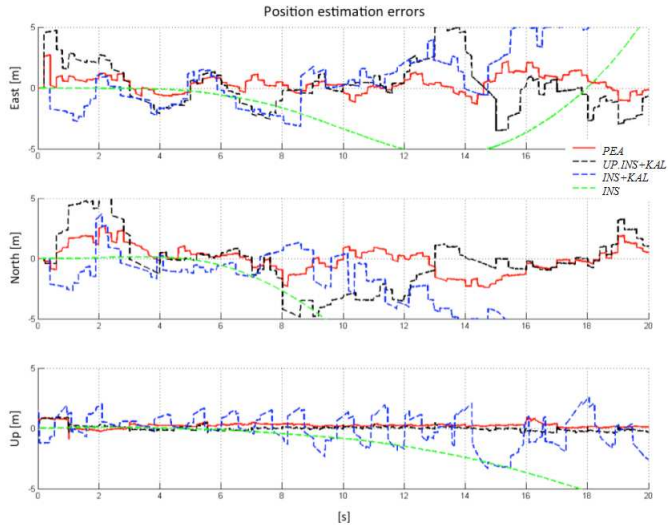

Fig. 8 Position estimation errors (coordinates in $\mathscr{R}_n$)

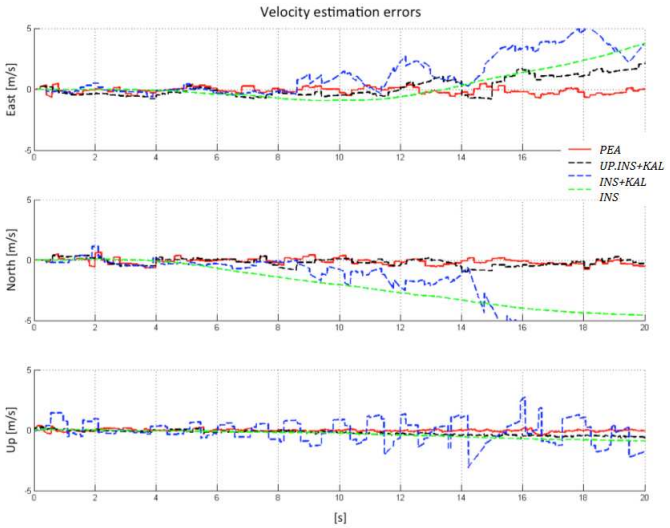

Fig. 9 Linear velocity estimation errors (coordinates in $\mathscr{R}_n$)

5.2.2 Rate gyros' and accelerometers' biases

The estimates of rate gyros' biases computed by the complementary filter are plotted in Figure 11. Estimation error never exceeds $\pm$5e-3 rad/s when steady state is reached, hence showing good accuracy. Note that whereas transient state lasts for about 2 to 4 sec on pitch and roll axes, it lasts for about 20 sec for the yaw axis.

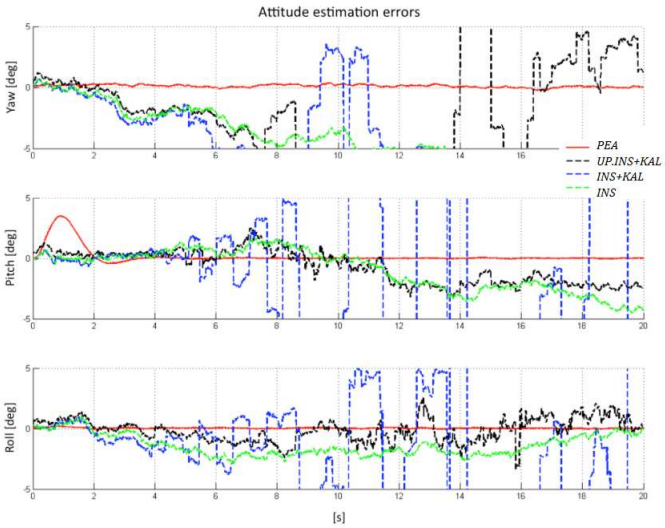

Fig. 10 Estimation errors on attitude angles

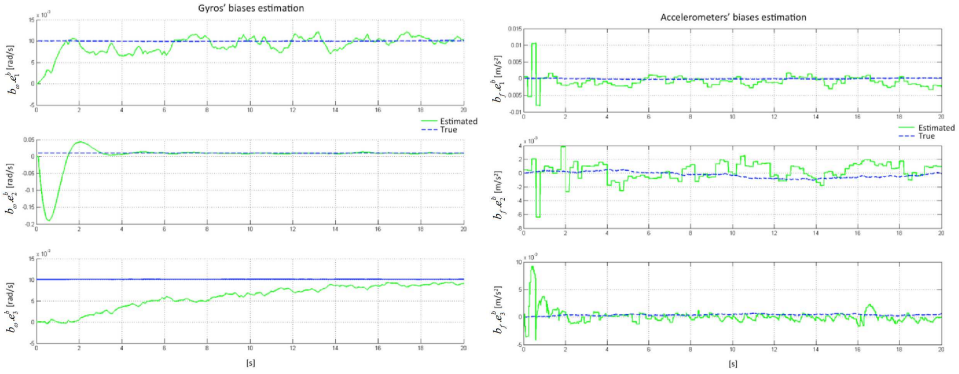

Fig. 11 Estimation of gyros' and acceleros' biases

This is an expected behaviour, as the UAV's yaw angle does not change much in this specific simulated trajectory. Indeed it can be shown that estimated parameters reach the true values only if the vertical direction "measured" by accelerometers and the horizontal direction "measured" by magnetometers change with time. Moreover, yaw axis gyro's bias estimation convergence takes more time if no second direction is provided (e.g. if magnetometers are subjected to strong perturbations).
Estimates of accelerometers' biases provided by the Kalman filter also prove to be accurate (see Figure 11), the estimation error never exceeding $\pm$3e-3 m/s^2 when steady state is reached.

5.3 Other results

In order to fully assess the performance of the proposed approach, several other simulations have been run. Three different trajectories have been considered: trajectory with small vertical and horizontal moves but with high increase in yaw angle, quasi-stationary flight with 360deg variation of yaw angle, trajectory with high variations of vertical and horizontal position components and small attitude angles. Each trajectory has been combined with the three following environment:

- Rural environment: free space, no close obstacles (hence no ultrasonic sensor is in reach, except for the vertical one for suitable altitudes), GPS fully available.
- Light urban environment: buildings along trajectory, GPS perturbed.
- Indoor environment: close obstacles including a roof, GPS unavailable.

Conclusions on the proposed approach performance are the following:

- Light urban type environment allows a quite nominal use of the whole set of sensors, and therefore leads to a state estimation quite insensitive to sensors' loss.
- Indoor environment is extremely sensitive to ultrasonic sensors loss, as they are the only way to get external position estimates (excepted from altitude provided by the baroaltimeter). In addition, perturbations on or loss of magnetometers' inputs lead to a coarsely estimated yaw angle, thus impacting horizontal position determination from ultrasonic sensors.
- In rural environment, unavailability of reliable GPS data (jamming, spoofing,) is damageable, as this sensor is the only one providing North and East positions, along with North, East and Down velocities. The altitude can still be coarsely estimated from baroaltimeter and/or vertical ultrasonic sensor when in range.

6 Conclusions

In this paper, an integrated system has been proposed for navigation of miniature rotorcraft-based UAVs in indoor and outdoor environments. Based on low-cost sensors, an hardware device has been developed for this study integrating IMU, baroaltimeter, GPS and ultrasonic sensors. An estimation architecture has been proposed to process the measurements provided by the sensors and estimate online the state of the vehicle (composed of its position, attitude and velocities). This architecture is based on a complementary filter for attitude estimation, and an INS and Kalman filter for position and linear velocity estimation from available measurements of several sensors. Procedures have been presented for selection of measurements. Processing of measurements provided by ultrasonic sensors has also been addressed, depending on the situation. Simulations results have been provided to illustrate the good performance of the proposed approach and its adaptability to various environments and robustness to perturbations and/or loss of sensors. Further work will

focus on real time implementation for flight experiments on a vehicle, and handling other perturbations such as mechanical vibrations.

References

1. A. Bachrach, R. He, and N. Roy. Autonomous flight in unknown indoor environments. *International Journal of Micro Air Vehicles*, 1(4):217 – 228, 2009.
2. M. Blösch, S. Weiss, D. Scaramuzza, and R. Siegwart. Vision based MAV navigation in unknown and unstructured environments. In *IEEE International Conference on Robotics and Automation*, pages 21 –28, 2010.
3. F. Caron, E. Duflos, D. Pomorski, and P. Vanheeghe. GPS/IMU data fusion using multisensor Kalman filtering: Introduction of contextual aspects. *Information Fusion*, 7(2):221–230, 2006.
4. J. Eckert, F. Dressler, and R. German. Real-time indoor localization support for four-rotor flying robots using sensor nodes. In *IEEE International Workshop on Robotic and Sensors Environments*, pages 23–28, 2009.
5. F. Fraundorfer, L. Heng, D. Honegger, G. Hee Lee, L. Meier, P. Tanskanen, and M. Pollefeys. Vision-based autonomous mapping and exploration using a quadrotor MAV. In *IEEE International Conference on Intelligent Robots and Systems*, pages 2997–3004, 2012.
6. M. George and S. Sukkarieh. Tightly coupled INS/GPS with bias estimation for uav applications. In *Australian Conference on Robotics and Automation*, 2005.
7. S. Grzonka, G. Grisetti, and W. Burgard. Towards a navigation system for autonomous indoor flying. In *IEEE International Conference on Robotics and Automation*, pages 2878 –2883, 2009.
8. D. Jung and P. Tsiotras. Inertial attitude and position reference system development for a small UAV. In *AIAA Infotech at Aerospace*. Rohnert Park, USA, 2007.
9. J. H. Kim and S. Sukkarieh. A baro-altimeter augmented INS/GPS navigation system for en uninhabited aerial vehicle. In *6th International Conference on Satellite Navigation Technology*. Melbourne, Australia, 2003.
10. R. Mahony, T. Hamel, and J.-M. Pflimlin. Nonlinear complementary filters on the special orthogonal group. *IEEE Transactions on Automatic Control*, 53(5):1203 –1218, 2008.
11. J. L. Marins, X. Yun, E. R. Bachmann, R. B. McGhee, and Zyda M. J. An extended Kalman filter for quaternion-based orientation estimation using MARG sensors. In *IEEE/RSJ International Conference on Intelligent Robots and Systems*, pages 2003–2011, 2001.
12. P. S. Maybeck. *Stochastic models, estimation and control, Volume 1*. Academic Press, 1979.
13. Najib Metni, Jean-Michel Pflimlin, Tarek Hamel, and Philippe Soueres. Attitude and gyro bias estimation for a VTOL UAV. *Control Engineering Practice*, 14(12):1511 – 1520, 2006.
14. N. Michael, D. Mellinger, Q. Lindsey, and V. Kumar. The GRASP multiple micro-uav testbed. *IEEE Robotics Automation Magazine*, 17(3):56 –65, 2010.
15. K. Schmid, F. Ruess, M. Suppa, and D. Burschka. State estimation for highly dynamic flying systems using key frame odometry with varying time delays. In *IEEE International Conference on Intelligent Robots and Systems*, pages 2997–3004, 2012.
16. B. Vik and T. I. Fossen. A nonlinear observer for GPS and INS integration. In *40th IEEE Conference on Decision and Control*, pages 2956–2961, 2001.
17. J. Wendel, O. Meister, C. Schlaile, and G. F. Trommer. An integrated GPS/MEMS-IMU navigation system for an autonomous helicopter. *Aerospace Science and Technology*, 10:527–533, 2006.
18. Ben Yun, Kemao Peng, and B.M. Chen. Enhancement of GPS signals for automatic control of a UAV helicopter system. In *IEEE International Conference on Control and Automation*, pages 1185 –1189, 2007.